Holographic light scattering in photorefractive crystals with local response

M. Goulkov and S. Odoulov
Institute of Physics, Science Ave 46, 03650, Kiev-39, Ucraine

Th. Woike
Institut für Mineralogie und Geochemie, Universität zu Köln, Zülpicherstrasse 49b, D-50674 Köln, Germany

J. Imbrock, M. Imlau, E. Krätzig, C. Bäumer, and H. Hesse
Fachbereich Physik, Universität Osnabrück, Barbarastrasse 7, D-49069 Osnabrück, Germany
(Received 9 October 2001; published 25 April 2002)

Strong polarization-isotropic wide-angle light scattering in photorefractive crystals with dominating photovoltaic response is explained referring to different experimental results obtained for $LiTaO_3$:Fe crystals. It is shown experimentally that the steady-state amplification of the light scattering results from a nonzero shift in the temporal frequency between the coherent optical noise and the pump beam. Competition of photovoltaic and diffusion contributions in the photorefractive effect leads to a spatial and temporal asymmetry of nonlinear scattering. Contributions of ''hot'' electrons in the diffusion process have to be assumed.

DOI: 10.1103/PhysRevB.65.195111 PACS number(s): 42.65.Hw, 42.70.Mp, 78.20.Jq

I. INTRODUCTION

Propagation of a laser beam in photorefractive crystals very often leads to the appearance of different patterns of scattered light known as photoinduced light scattering[1] or beam fanning.[2] This nonlinear phenomenon is the result of beam-coupling processes when a seed radiation is amplified at the expense of the incident beam. The incident beam is partially scattered from surface and bulk optical inhomogeneities randomly distributed in the crystal. This primary scattered light interferes with the transmitted beam, forming a continuous set of elementary light patterns. Because of the photorefractive effect[3] the light modulation records elementary ''noisy'' gratings of the refraction index (index gratings) in the volume of photorefractive crystals. If index gratings are spatially shifted with respect to the original light modulation, the diffraction of the laser beam from the gratings may result in an amplification of the seed waves. The wide-angle pattern of such a photoinduced light scattering develops in the directions where nonlinear wave mixing ensures efficient energy transfer. The particular mechanisms of the photorefractive nonlinearity are different for different crystals providing a rich variety of scattering processes. The study of photoinduced scattering helps to understand the processes of light amplification in the particular photorefractive crystal.

A satisfactory model of wide-angle scattering has been developed up to now only for crystals with purely nonlocal response, particularly with dominating diffusion mechanism of the space-charge transport such as undoped $LiNbO_3$ and $LiTaO_3$, $BaTiO_3$ and SBN.[1,2] This model considers the frequency-degenerated case in which the temporal frequencies of incoming and scattered light are identical leading to a standing light modulation. Thus, the noisy index gratings are exactly $\pi/2$-phase shifted with respect to the light modulation and this shift ensures optimal conditions for stationary energy exchange only in one direction (either against or along the polar *c* axis depending on the sign of the photocarriers and on the sign of the electro-optic coefficient). As a result, the propagation of a single laser beam in *X*- or *Y*-cut samples always yields here one-sided scattering patterns. Properties of the scattering in undoped $LiNbO_3$ and $LiTaO_3$ are in good qualitative agreement with the theory of photoinduced scattering in crystals with pure nonlocal response.[4]

At the same time, the model of the scattering based on the diffusion nonlinearity is not able to describe the properties of polarization-isotropic scattering observed in $LiTaO_3$ and $LiNbO_3$ crystals doped with iron or copper. Particularly, the anomalous brightness and the two-sided shape of the scattering pattern observed in doped crystals cannot be explained in the frame of this model. According to Refs. 5 and 6 the dominating space-charge transport in doped $LiTaO_3$ and $LiNbO_3$ is a photovoltaic effect and the photorefractive response is local, resulting in unshifted index gratings (we restrict here our consideration to polarization-isotropic scattering where incident and scattered light are identically polarized). Thus, no stationary intensity coupling between seed and pump waves should occur and no strong photoinduced scattering is expected via the photovoltaic nonlinearity. Only some transient scattering is allowed because of a bend of the fringe pattern if a phase transfer between two interacting waves occurs.[7]

The first attempt to exceed the limits of the traditional model of frequency-degenerate scattering was made in Ref. 8, where a nonzero shift in the temporal frequency of the scattered light is considered as the necessary condition for its effective amplification in crystals with local response. Some experimental evidence for frequency detuning in photoinduced scattering is presented in Refs. 9 and 10, but up to now no satisfactory theory has been developed that explains the properties of wide-angle scattering in doped $LiTaO_3$ and $LiNbO_3$ crystals in all details.

In this paper we present different experimental results on photoinduced wide-angle scattering in $LiTaO_3$:Fe crystals with a photovoltaic response. Clear experimental evidence of the temporal frequency shift in wide-angle light scattering in

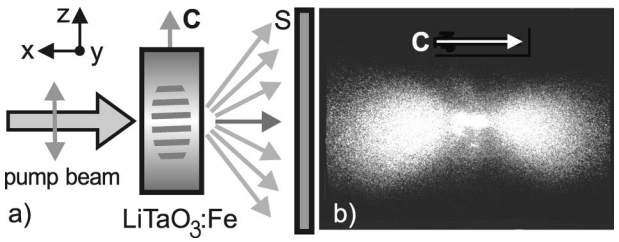

FIG. 1. (a) Schematic representation of the experimental setup with $LiTaO_3$:Fe; (b) Far-field scattering pattern on the screen *S*.

$LiTaO_3$:Fe crystal is reported. The asymmetry of the scattering pattern is measured and analyzed. It is found that the temporal evolution as well as the frequency detuning of the scattered light is different for directions along and against the polar axis of the crystal. Based on the experimental results we discuss the qualitative model of isotropic scattering taking into consideration the following key assumptions. We consider, (1) the case of frequency-nondegenerate scattering,[8,11] (2) the competiton of photovoltaic and diffusion contributions to light amplification processes,[12] (3) the contribution of ''hot'' (nonthermalized) electrons in the diffusion space-charge transport.[13] We show that these three model assumptions are able to explain qualitatively all features of the photoinduced scattering measured in $LiTaO_3$:Fe crystals. The theoretical dependence of the coupling strength on the frequency shift is calculated for the quantitative explanation of some scattering properties.

II. EXPERIMENTAL RESULTS

An *a*-cut sample of $LiTaO_3$:Fe (800 wt% ppm Fe) of $a \times b \times c = 3.4 \times 1.85 \times 4.3$ mm^3 dimensions with the *c* axis aligned in the table plane is illuminated by the light of an Ar-ion laser operating at the wavelength $\lambda = 514$ nm. An unexpanded extraordinarily polarized laser beam of 2.2 mm diameter impinges on the crystal perpendicularly to the *YZ* surface [see Fig. 1(a)]. In order to avoid undesirable pyroelectric charges on the crystal surfaces during its exposure to coherent light,[14,15] the crystal is immersed in a cell with a soft alkaline solution. Bright photoinduced light scattering develops when the pump beam starts to illuminate the crystal. The transmitted pump beam is strongly depleted because of the scattering processes, in the steady state the total scattering intensity reaches a value of the same order of magnitude as the pump beam intensity.

Figure 1(b) shows a scattering pattern on a screen *S* placed behind the crystal. The bright spot in the middle of the screen corresponds to the pump beam. Scattered light arising mostly in the *XZ*-plane forms the wide-angle pattern on the screen, consisting of two bright diffuse strips, one oriented in the direction of the *c* axis of the crystal (''$+c$'' strip) and the other in the opposite direction (''$-c$'' strip). The well-pronounced two-sided shape of the scattering pattern is typical for doped $LiNbO_3$ and $LiTaO_3$ crystals,[18] whereas in undoped crystals the pattern always has one-sided shape (unidirectional beam fanning). The polarization of the scattered light in Fig. 1(b) is identical to the polarization of the pump beam (extraordinary scattered waves).

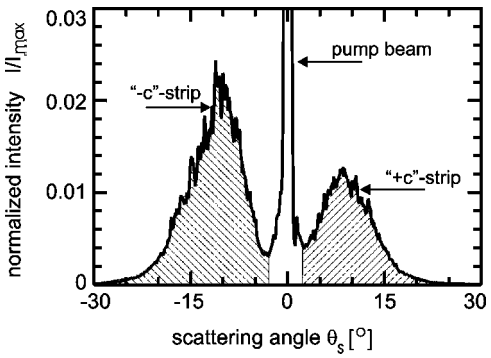

FIG. 2. Angular intensity distribution of scattered light in *XZ* plane. The central peak corresponds to the transmitted pump beam.

The scattering pattern exhibits an asymmetry in the intensity distribution, the ''$+c$'' strip is weaker than the ''$-c$'' strip. Figure 2 shows a scan of the angular distribution of the steady-state light intensity measured in the *XZ* plane. The scattering angle θ_s is the angle measured from the pump beam to the current position of the photodiode, positive and negative angles correspond to the $+c''$ and the $-c$ direction, respectively. The computer controlled angular displacement of the photodiode is discrete with $\Delta\theta_s = 0.1°$ between two adjacent positions. The scattered light collected by the photodiode aperture forms a cone with an apex angle of $\delta\theta_{pd} = 0.3°$ (photodiode aperture angle). The measured total intensity of the scattered light in the $-c$ strip is about two times larger than that in the $+c$ strip, $I^{\Sigma}_{-c}/I^{\Sigma}_{+c} \approx 2$ (I^{Σ}_{-c} and I^{Σ}_{+c} are two crosshatched regions under the experimental curve shown in Fig. 2 and separated by the central pump beam peak). The maximum of the scattering intensity in the $-c$ and in the $+c$ strip of the scattering pattern is found at $\theta_s^{-c} = -12°$ and $\theta_s^{+c} = +8°$, respectively. A rotation of the crystal by 180° around the *Y* axis resulting in the inversion of the *c* axis leads to a redistribution of the scattered light in such a way that the $-c$ strip is again brighter than the $+c$ strip.

The study of the scattering dynamics shows the following results. Figure 3 presents the temporal development of the scattering measured for the $+c$ and the $-c$ strip (two solid curves) from the beginning to the steady state. Two photodiodes are placed symmetrically with respect to the direction

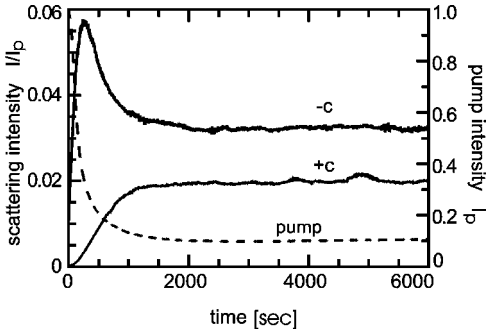

FIG. 3. Temporal development of scattered light (solid lines) and depletion of the pump beam (dashed line). $\theta_s = \pm 12°$, $I_p = 0.26$ W/cm^2, $\delta\theta_{pd} = 6°$.

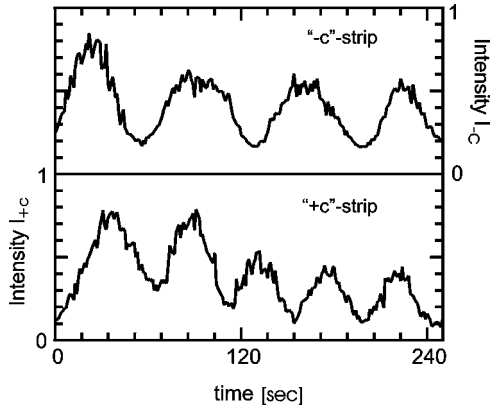

FIG. 4. Intensity dynamics of a single pixel of the scattering pattern (a) in "$+c$"-strip and (b) in "$-c$"-strip. The crystal is preliminary illuminated by the pump beam for a time $t \gg \tau_{di} \cdot \theta_s = \pm 12°$, $I_p = 1.6$ W/cm^2, $\delta\theta_{\mathrm{pd}} = 0.015°$.

of the pump beam and are adjusted under an angle of $\theta_s = \pm 12°$. The pump beam intensity is $I_p = 0.26$ W/cm^2. The curves are taken with the largest possible aperture angle $\delta\theta_{\mathrm{pd}} = 6°$ in order to measure the integral response from a large number of elementary pixels of the scattering pattern. Two curves clearly indicate the main difference in the temporal evolution of the scattering in the two directions. The $-c$ scattering exhibits a well-pronounced transient intensity peak before the steady state is reached, while there is no transient peak for the $+c$ scattering. The dashed curve on Fig. 3 illustrates the pump beam depletion that is due to the scattering process.

To study the temporal behavior of a single pixel of the light pattern, the dynamics is measured after the crystal has been already exposed for a quite long time $t \gg \tau_{di}$ (steady state), where τ_{di} is the dielectric relaxation time. These measurements are performed at the scattering angles of $\theta_s = \pm 12°$, but with the aperture angle of the photodiodes reduced to $\delta\theta_{\mathrm{pd}} = 0.015°$. The resulting curves (one for the $+c$ and the other for the $-c$ side) are shown in Fig. 4 and exhibit periodic variations of the scattering intensity with different beat frequencies for the $+c$ and the $-c$ strip. The period T_b of the intensity modulation is dependent on the pump intensity and decreases for increasing I_p. However, the ratio $\mathrm{T}_b^{+c}/\mathrm{T}_b^{-c}$ remains constant. Figure 5 shows the measured dependence of the beat frequency $\Omega_{\pm c} = 2\pi/\mathrm{T}_b^{\pm c}$ vs the pump intensity. It should be noted that the crystal is always immersed in the alkaline solution. For a crystal in air the dynamics become irregular because of a surface electrical breakdown imposed upon the periodic beatings. An increasing of the aperture angle of the photodetector also leads to a gradual decrease of the intensity modulation until its complete disappearance.

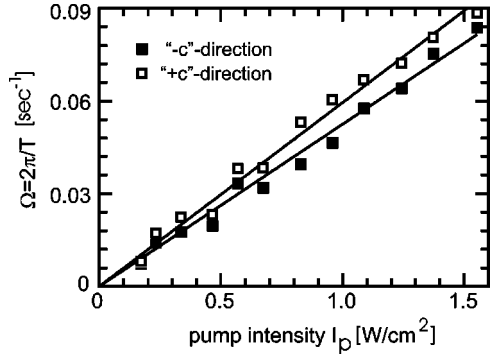

FIG. 5. Temporal frequency of the intensity of a single pixel in the scattered light vs the pump beam intensity. $\theta_s = \pm 12°$.

This effect of the vanishing of the periodical variations with increasing aperture angle observed in the experiment can be explained if the stochastic nature of primary scattering is taken into account. Elementary interference patterns formed by transmitted light with different seed waves are not correlated in phase. An enlargement of the aperturte angle increases the number of stochastically independent noise components contributing to the photodetector input. When the aperture angle exceeds some limiting value the averaged signal becomes irregular.

III. DISCUSSION

To explain the features of the scattering observed in our experiments we first accept the following basic assumptions.

(1) We assume the existence of a nonzero shift in the temporal frequency between the scattered and the pump waves and nearly degenerate photorefractive coupling in this case is considered. For example, the part of the initial seed scattering characterized by the temporal frequency ω_s can be slightly shifted with respect to the fundamental frequency ω_p of the laser radiation.[8,11] The frequency spectrum of the primary scattering is a Lorenz function and the optimal frequency detuning is described by the reciprocal dielectric relaxation time, $\Omega = \omega_p - \omega_s = 1/\tau_{di}$.

(2) Next, we point out the principal necessity to account for contributions of both photovoltaic and diffusion charge transport in the coupling of the scattered waves and the pump wave.

(3) We also allow a contribution of nonthermalized electrons in the diffusion process.

Below, we consider the interaction of the transmitted component p of the pump beam with the light field $\mathcal{E}_p = \mathcal{E}_p^0 \exp[-i(\mathbf{k}_p\mathbf{r} - \omega_p t - \phi_p)]$ and the scattering component s with the field $\mathcal{E}_s = \mathcal{E}_s^0 \exp[-i(\mathbf{k}_s\mathbf{r} - \omega_s t - \phi_s)]$, where $\mathbf{k}_p$ and $\mathbf{k}_s$ are wave vectors, and ϕ_p and ϕ_s are initial phases. An interference of these two waves results in an elementary light modulation $I = I_0[1 + m\cos(\mathbf{K}\mathbf{r} + \Omega t + \Delta\phi)]$, where $\mathbf{K} = \mathbf{k}_s - \mathbf{k}_p$ is the light modulation wave vector ($|\mathbf{K}| = 2\pi/\Lambda$), $\Delta\phi = \phi_p - \phi_s$, $I_0 = I_s + I_p$ is the total intensity and $m = 2\mathcal{E}_p^0\mathcal{E}_s^0/I_0$. This parasitic elementary light modulation produces an electric space-charge field by charge migration, recording phase gratings by the modulation of the refractive index (index grating) via the linear electro-optic effect, $\Delta n = \frac{1}{2} r_{eff} n^3 E_{sc}$, where n is the refractive index, r_{eff} is the effective electro-optic coefficient, and E_{sc} is the electric space-charge field. If the parasitic index gratings are phase shifted with respect to the light modulation, stationary intensity coupling takes place and the scattered light is amplified at the expense of the pump beam.

The efficiency of the amplification process is described by the coupling strength γl, constituted of the product of crystal thickness l and coupling constant $\gamma = 2\pi\Delta n\lambda^{-1}$ that specifies the nonlinear properties of the crystal.[3] It is assumed that in the general case the coupling constant is complex, $\gamma = \gamma' + i\gamma''$, where real and imaginary parts describe phase and amplitude exchange between two waves, respectively. Thus, the exchange of amplitudes corresponds to stationary amplification of scattering, but the phase exchange between the s and p waves results only in a transient amplification caused by the inertial properties of the nonlinear media. The type of the photorefractive nonlinearity is divided into a nonlocal response ($\gamma'' \neq 0, \gamma' = 0$) and a local response ($\gamma'' = 0, \gamma' \neq 0$) and strongly depends on the processes of charge migration forming the electric field.

For doped $LiTaO_3$ (as well as for doped $LiNbO_3$), electrons are the major photocarriers for excitation with visible light.[19] We admit a dominating role of the photovoltaic effect in the processes of formation of the electric space-charge field. The photovoltaic electric field exhibits strong spatial anisotropy[19]

$$E^{pv}(r) = \frac{\beta_{eff}}{\kappa}\cos(\mathbf{Kr} + \Omega\tau + \Delta\phi), \tag{3.1}$$

where κ is the specific photoconductivity, β_{eff} is the component of the photovoltaic tensor that describes the anisotropic properties of the photovoltaic effect. The largest components of the β tensor for $LiTaO_3$ are $\beta_{333} \approx \beta_{311} = \beta_{322}$, resulting in most efficient recording of parasitic gratings in $\pm c$ direction. The photovoltaic electric field measured for our particular $LiTaO_3$ sample along the c axis is about 84 kV/cm for illumination with light of 514 nm wavelength.

Diffusion is considered in our scattering model as an important additional charge transport. Acording to Ref. 16, the diffusion electric field can be written as

$$E^{dif}(r) = \frac{(k_B T/e)K + m_d(\epsilon_h/e)K}{1 + m_d}\sin(\mathbf{Kr} + \Omega\tau + \Delta\phi), \tag{3.2}$$

where e is the elementary electric charge, k_B the Boltzman constant, and T the absolute temperature. The first term in the numerator is due to the diffusion of thermalized electrons (E_T^{dif}). The second term (E_N^{dif}) describes the electric field formed via diffusion of photoexcited electrons with energies ϵ_h higher than the typical energy of thermal activation ($\epsilon_h > k_B T$). Such electrons usually are called ''hot'' or nonthermalized electrons. The parameter m_d in Eq. (3.2) determines the ratio between these two contributions. In the case of $m_d \ll 1$ the diffusion of thermalized electrons is dominating and for $m_d \gg 1$ the contribution of hot electrons is important. An intermediate value of m_d corresponds to a share holding of electrons of both types in the diffusion charge transport. Keeping in mind that the scattering intensity has a maximum at a spatial period of $\Lambda = 5\ \mu$m, the diffusion field owing to thermalized electrons reaches $E_T^{dif} = 1.3$ kV/cm. A contribution of nonthermalized electrons estimated from independent beam-coupling and scattering experiments[12,13] gives values for E_N^{dif} in the range of 4 to 20 kV/cm that significantly exceed E_T^{dif}.

In the frequency-degenerate case ($\omega_s = \omega_p$), according to Eq. (3.1), the photovoltaic space-charge transport corresponds to a local response and results in no stationary beam coupling between scattered and transmitted parts of the laser beam. On the other hand [see Eq. (3.2)], diffusion provides a nonlocal response with a spatial $\Lambda/4$ shift of the index grating in the $-c$ direction ($\pi/2$-phase mismatch) with respect to the light modulation and consequently the amplified scattered light is oriented only in this direction. The typical value of the coupling strength calculated for $LiTaO_3$ crystal with the help of Eq. (3.2) ranges only up to $\gamma'' l = 4$ that is too small to explain the anomalously bright scattering observed in the experiment.

Now, let us assume that temporal frequencies of the transmitted and scattered wave are different ($\omega_s \neq \omega_p$). In this case the interference pattern formed by the p and the s wave will run in space with a speed $\nu = 2\pi\Omega/K$. Because of its inertial properties, the medium is in delay with the response of the moving interference pattern so that the index grating is permanently shifted with respect to the light modulation. Intensity coupling becomes possible and the direction of energy transfer depends on the sign of frequency detuning Ω. The coherent light with $\omega_s < \omega_p$ is amplified. Thus, the presence of a running light modulation withdraws the prohibition of stationary energy transfer between the two coherent waves in photorefractive media with initially local response.

The presence of frequency-shifted components in the scattered light is demonstrated by the dynamics of a single pixel of the scattering pattern in Fig. 4. We suppose that the periodic variations of the scattering intensity depict a spatial movement of the elementary interference pattern formed by one of the frequency-shifted components (elastic scattering, $\omega_s^e \neq \omega_p$) with the frequency-degenerate component (inelastic scattering, $\omega_s^i = \omega_p$). The beating period T_b depends on the frequency detuning value $\Omega = 2\pi/T_b$.

The bidirectional shape of the scattering patterns enables us to suggest, that the sign of Ω is the same for the $+c$ and the $-c$ direction, allowing the grating moving from the pump beam in both directions. The reciprocal values of the average detuning $\tau = 2/(\Omega_{+c} + \Omega_{-c})$ calculated from the data of Fig. 4 are close to the values of the dielectric relaxation time τ_{di} measured directly from holographic experiments for the same range of pump intensities in agreement with the model assumption of $\Omega\tau_{di} = 1$. The differences in the frequency shift ($\Delta\Omega = \Omega_{+c} - \Omega_{-c}$) observed for the two directions (see Fig. 5) result in different phase shifts between index and light gratings, and consequently in different amplification rates of the seed scattering in these directions.

The assumption of a nonzero frequency shift in photoinduced scattering for crystals with local response is also confirmed by the experimental observation of the beat frequency in the scattering intensity in $LiNbO_3$:Fe crystals.

Taking into account a nonzero frequency detuning Ω in the scattered light, the expressions for the coupling coefficents of the photovoltaic and diffusion contributions can be represented[17] as

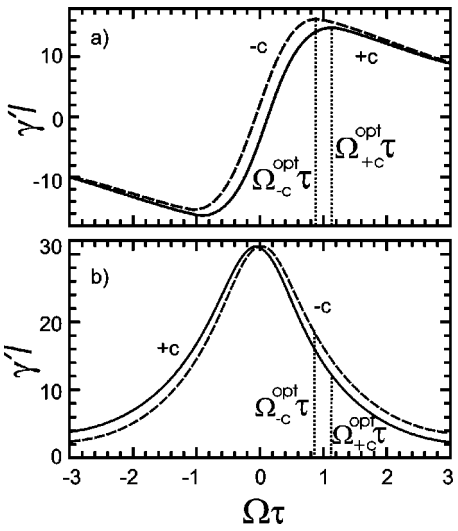

FIG. 6. Coupling strength γl vs $\Omega\tau$. (a) Im$\{\gamma l\}$; (b) Re$\{\gamma l\}$. $E^{pv}=84$ kV/cm, $E^{dif}=5.4$ kV/cm, $\Delta\Omega^{opt}\tau=0.14$.

$$\gamma^{pv}=\frac{\gamma_0^{pv}}{1+(\Omega\tau)^2}+i\frac{\gamma_0^{pv}\Omega\tau}{1+(\Omega\tau)^2}, \tag{3.3}$$

$$\gamma^{dif}=\frac{\gamma_0^{dif}\Omega\tau}{1+(\Omega\tau)^2}+i\frac{\gamma_0^{dif}}{1+(\Omega\tau)^2}, \tag{3.4}$$

where $\gamma_0^{pv}=\pi n^3 r_{eff}E^{pv}/\lambda$ and $\gamma_0^{dif}=\pi n^3 r_{eff}E^{dif}/\lambda$. For our particular case of extraordinary waves and grating wave vectors oriented closely to the c axis, $n\approx n_e$, $r_{eff}\approx r_{333}$.

The additional phase shift that results from the frequency detuning is smaller than the diffusion shift. Hence, even for the frequency nondegenerated case, the diffusion response contributes to amplification only in one direction (against the c axis in $LiTaO_3$), in the opposite direction the scattering is depleted. For an initially local photovoltaic response, the presence of frequency detuning Ω gives rise to an amplification of the scattered light equal in the $+c$ and in the $-c$ direction. Thus, values γ^{pv} and γ^{dif} should be added in the $-c$ direction and subtracted in the $+c$ direction, resulting in different values of $\gamma_{\pm c}$. The final expressions for the imaginary and the real part of the coupling coefficient are

$$\gamma''=\frac{\pi n^3 r_{333}}{2[1+(\Omega\tau)^2]}(\Omega\tau E^{pv}\pm E^{dif}), \tag{3.5}$$

$$\gamma'=\frac{\pi n^3 r_{333}}{2[1+(\Omega\tau)^2]}(E^{pv}\pm\Omega\tau E^{dif}), \tag{3.6}$$

where the sign "+" is valid for the "$-c$" direction, and the sign "−" for the "$+c$" direction. Figure 6(a) shows the calculated dependence of $\gamma'' l$ vs $\Omega\tau$ and depicts the important fact that the coupling strength $\gamma'' l$ reaches its maximum at different $\Omega^{opt}\tau$ values for the $+c$- and the $-c$-direction. In other words, the optimal frequency detuning is different for the two sides of the scattering pattern and $\Delta\Omega^{opt}=\Omega^{opt}_{+c}-\Omega^{opt}_{-c}>0$. The last conclusion is in agreement with our experimental results (see Figs. 4 and 5). The theoretical result $\gamma''_{-c}l>\gamma''_{+c}l$ explains the asymmetry in the angular light distribution, shown in Fig. 2. Noticeably large values of $\gamma'' l$ also explain the anomalous brightness of the scattering pattern that is much stronger than the scattering in undoped $LiTaO_3$.

Another important conclusion from Fig. 6(a) is the following: The calculation of the two curves in Fig. 6(a) is based on the assumption that the theoretical value $\Delta\Omega^{opt}\tau$ should fit the experimental value $\Delta\Omega\tau=0.14$ taken from Fig. 5. The best correspondence of the relative shift $\Delta\Omega\tau$ of the maximum of the theoretical curves $\gamma'_{-c}l(\Omega\tau)$ and $\gamma'_{+c}l(\Omega\tau)$ to the experiment data is for the value of the diffusion field of $E^{dif}=5.6$ kV/cm, that is much larger than the electric field E_T^{dif} produced by the diffusion of thermalized electrons, $E^{dif}/E_T^{dif}=4.3$. Using the value of $E_T^{dif}=1.3$ kV/cm (typical for $LiTaO_3$) in Eq. (3.5) would result in an equal frequency shift Ω^{opt} and, therefore, in an equal $\gamma'' l$ value for the two directions, in contradiction to the experiment. On the other hand, the obtained ratio 4.3 is in a good agreement with results of independent measurements.[12,13] Thus, this result of our experiments can also serve as an argument in favor of the assumption of a considerable contribution of nonthermalized electrons in diffusion processes in $LiTaO_3$.

The theoretical dependence of $\gamma' l$ on $\Omega\tau$ shown in Fig. 6(b) gives us the possibility to explain the differences in the temporal evolution of the scattered light in the $+c$ and the $-c$-strip (Fig. 3). Since the real part of the coupling strength is responsible for the transient amplification of the scattered light,[7] the presence of a nonzero frequency detuning results also in an asymmetry of the process of transient amplification of scattered light. A difference in the value of Ω^{opt} in the $+c$ and in the $-c$-direction causes different shifts of the optimal $\gamma' l$ from the corresponding theoretical maxima. The difference between $\gamma'_{+c}l$ and $\gamma'_{-c}l$ is not proportional to the difference between $\gamma''_{+c}l$ and $\gamma''_{-c}l$. For our particular case of $LiTaO_3$ crystals, $\gamma'_{-c}l>\gamma''_{-c}l$ and $\gamma'_{+c}l<\gamma''_{+c}l$, meaning that only in the $-c$ direction the transient amplification exceeds the amplification in the steady state. The exceeding of $\gamma' l$ over $\gamma'' l$ in the $-c$ direction causes a transient intensity peak in the scattering dynamics defined by $\gamma' l$. After that the intensity decreases to the steady-state level defined by $\gamma'' l$. On the other hand, no transient scattering peaks should be observed in the $+c$-direction. A larger contribution of diffusion to the electric space-charge field will result in an increase of $\Delta\Omega\tau$, so that the transient peak for scattering in the $-c$ strip should be more pronounced.

IV. CONCLUSIONS

Experiments were carried out with $LiTaO_3$:Fe to study the photoinduced light scattering in photorefractive crystals with dominating photovoltaic response. The presented model of polarization-isotropic wide-angle scattering is considered to explain both, dynamics and steady-state properties of the scattering pattern observed in the experiments. It is proved that anomalously bright polarization-isotropic scattering in $LiTaO_3$:Fe originates from frequency-shifted components of

the scattered light nonlinearly amplified at the expense of pump beam. The asymmetry in the intensity distribution and in the dynamics of the scattering results from the competition of contributions of the diffusion and the photovoltaic effect in the charge transport processes. The presented results support also the significant role of diffusion of nonthermalized electrons in processes of the spatial redistribution of photocarriers.

ACKNOWLEDGMENTS

This work was supported by the Deutsche Forschungsgemeinschaft within the framework of the Schwerpunktprogramm SPP 1056: ''Strukturgradienten in Kristallen'' (Project No. WO 618/3-2). One of us (M.G.) acknowledges support from D.F.G. for his stay in the Institut für Mineralogie, Universität zu Köln.

[1] V. V. Voronov, I. R. Dorosh, Yu. S. Kuzminov, and N. V. Tkachenko, Kvant. Elektron. **7**, 2313 (1980) [Sov. J. Quantum Electron. **10**, 1346 (1980)].
[2] J. Feinberg, J. Opt. Soc. Am. **72**, 46 (1982).
[3] N. V. Kukhtarev, V. P. Markov, S. G. Odoulov, M. S. Soskin, and V. L. Vinetskii, Ferroelectrics **22**, 961 (1979).
[4] V. V. Obukhovski and A. V. Stoyanov, Kvant. Elektron. **12**, 563 (1985) [Sov. J. Quantum Electron. **15**, 367 (1985)].
[5] D. von der Linde and A. M. Glass, Appl. Phys. **8**, 85 (1975).
[6] E. Krätzig and R. Orlowski, Ferroelectrics **27**, 241 (1980).
[7] N. V. Kukhtarev, V. B. Markov, and S. G. Odoulov, Sov. Phys. Tech. J **25**, 1109 (1980).
[8] B. I. Sturman, Zh. Eksp. Teor. Fiz. **100**, 1071 (1991) [Sov. Phys. JETP **73**, 593 (1991)].
[9] B. Sturman, M. Goulkov, and S. Odoulov, Appl. Phys. B: Photophys. Laser Chem. **B56**, 193 (1993).
[10] E. Shamonina, B. I. Sturman, S. G. Odoulov, and K. H. Ringhofer, J. Opt. Soc. Am. B **13**, 2242 (1996).
[11] H. C. Pedersen, P. E. Andersen, and P. M. Johansen, Opt. Lett. **20**, 2475 (1995).
[12] V. L. Vozniy, V. V. Lemeshko, V. V. Obukhovski, and A. V. Stoyanov, Ukr. Phys. J. **34**, 652 (1989).
[13] V. G. Brovkovich and B. I. Sturman, Pis'ma Zh. Eksp. Teor. Fiz. **37**, 464 (1983) [Sov. Phys. JETP **37**, 550 (1983)].
[14] E. S. Vartanyan, R. K. Ovsepyan, Kvant. Elektron. **6**, 2455 (1979) [Sov. J. Quantum Electron. **9**, 1449 (1979)].
[15] V. V. Bryksin, O. V. Kandidova, L. I. Korovin, V. V. Lemanov, and B. V. Sukharev, Sov. J. Tech. Phys. **56**, 2353 (1986).
[16] B. I. Sturman and V. M. Fridkin, *The Photovoltaic and Photorefractive Effects in Noncentrosymmetric Materials* (Gordon and Breach, Philadelphia, 1992).
[17] S. G. Odoulov, M. S. Soskin, and A. I. Khyzniak, *Dynamic Grating Lasers* (Harwood, London, 1991).
[18] R. A. Rupp, J. Marotz, K. H. Ringhofer, S. Treichel, S. Feng, and E. Krätzig, IEEE J. Quantum Electron. **23**, 2136 (1987).
[19] R. Orlowski and E. Krätzig, Solid State Commun. **27**, 1351 (1978).